ADVANCED FUNCTIONAL MATERIALS
www.afm-journal.de

Materials Views
www.MaterialsViews.com

Enhancing the Cellular Delivery of Nanoparticles Using Lipo-Oligoarginine Peptides

*Jae Sam Lee and Ching-Hsuan Tung**

Nanoparticles have great potential as nanotherapeutics, delivery vectors, and molecular imaging agents due to their flexible properties. Although intracellular and nuclear delivery of nanoparticles is desirable for therapeutic applications, it remains a challenge. Cell penetrating peptides (CPPs) are a powerful tool for the intracellular delivery of various cargoes. Here it is reported that functionalization of nanoparticles with a myristoylated oligoarginine CPP promotes cellular uptake without increased toxicity. It is evident that the myristoylated CPP is much more effective in transporting nanoparticles than the unmodified CPPs.

1. Introduction

Nanoparticles (NPs) have gained attention in therapeutic and biomedical applications due to excellent physical and chemical properties that arise from their small size (<100 nm) and high surface-to-volume ratio.[1–3] Various biomedically relevant NPs have been reported, including polymeric NPs, metal NPs, and quantum dots.[4–7] Among these, gold nanoparticles (AuNPs) have been investigated as attractive candidates for cell trafficking, targeted drug delivery, hyperthermia cancer therapy, and molecular imaging contrast agents. AuNPs easily conjugate to biomolecules, exhibit low toxicity, and have excellent optical and physical properties that are dependent on their size, surface layer, and shape.[1,8–10] Numerous functionalized AuNPs (fAuNPs) have been developed by surface coating with peptides, proteins, oligosaccharides, and nucleic acids. Therefore, AuNPs can exert their desired therapeutic effect on targets and be multifunctional for therapeutic and diagnostic applications.[11–13] Cellular uptake of NPs is dependent on size, shape, and surface charge.[2,10,12,14] For instance, 30 to 70 nm AuNPs can enter cells by non-specifically adsorbing serum proteins onto their surfaces and the proteins then facilitate entering into the cell via surface receptors. The shape of NPs indeed plays an important role in the cellular uptake. Cells take up fewer rod-shaped AuNPs than spherical AuNPs, which may be due to differences in curvature that affect the contact area with cell membrane receptors. Likewise, the surface charge of NPs also influences cellular localization and the toxicity profile.[3,15,16]

Dr. J. S. Lee, Prof. C. H. Tung
Department of Translational Imaging
The Methodist Hospital Research Institute
Weill Cornell Medical College
6565 Fannin, B5-009, Houston, TX 77030, USA
E-mail: ctung@tmhs.org

DOI: 10.1002/adfm.201201345

Most AuNPs taken up by cells via endocytosis are trapped inside endosomal vesicles unless they are introduced into cells by other disruptive methods. Recent studies have shown that modification of AuNPs with liposomes or cell penetrating peptides (CPPs) as delivery vectors can avoid the endosomal pathway.[17–19] CPPs can facilitate the translocation of various cargoes into cells, such as peptides, proteins, and molecular imaging reporters;[7,12,17,20–23] moreover, CPPs are also efficient vectors to deliver various NPs,[6,24] including AuNPs.[25] Of the reported CPPs, arginine-rich peptides are particularly interesting because of their high cellular uptake efficiency. The guanidine moiety in arginine-rich peptides plays a crucial role in translocation through the plasma membrane.[23,26,27] Recent reports also determined that a hydrophobic moiety conjugated to CPPs can further improve cellular uptake efficiency.[28–34]

Previously, we developed lipo-oligoarginine peptides (LOAPs) by conjugating a proper combination of hydrophobic fatty acids and positively charged oligoarginines, which enhanced the cellular uptake of cargo into cells.[30–32] One particular LOAP, myristoylated hendeca-D-arginine peptide (MLP, **Figure 1**), exhibited the most reliable results for elevated cellular uptake rate, intracellular localization, low cellular toxicity, and enhanced metabolic stability.[31] Therefore, we prepared functionalized AuNPs (fAuNPs) by incorporating MLP on their surfaces to improve cellular uptake rate and intracellular trafficking with minimal cellular toxicity. For comparison, acetylated hendeca-D-arginine peptides (ALP, Figure 1) were included as a control and to study the contribution of the lipophilic myristoyl group. The physicochemical and optical properties of the fAuNPs were characterized using MALDI-TOF mass spectrometry, UV-visible spectroscopy, dynamic light scattering, and ζ-potential. Cellular uptake and intracellular distribution of fAuNPs in Jurkat cells were evaluated by flow cytometry and confocal laser scanning microscopy (CLSM). Cell viability was quantified by MTS assay and by calcein red-orange dye flow cytometric analyses. Finally, the intracellular fate of AuNPs was examined in MDA-MB-231 breast cancer cells by dark-field microscopy and hyperspectral microscopy.

2. Results and Discussion

2.1. Synthesis of LOAPs and Conjugation to AuNPs

LOAPs were synthesized by conventional Fmoc chemistry as previously reported (see also Supporting Information, Scheme S1).[30–32] ALP and MLP were purified from preparative

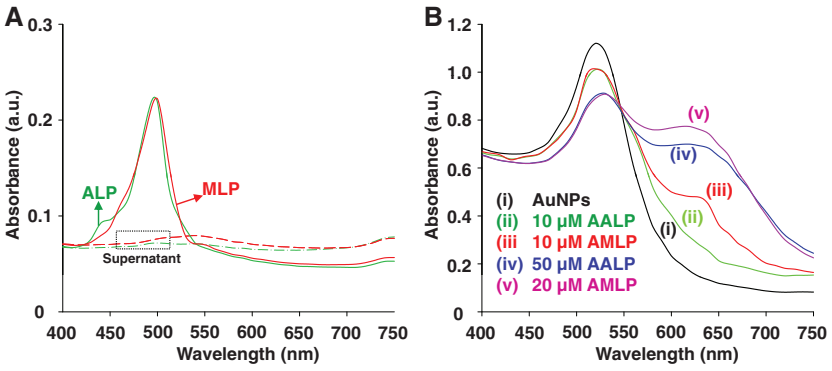

C

Name	Particle Size (nm)[a]	Zeta Potential (mV)[a]
AuNP	20.2 ± 0.7	-38.8 ± 2.3
AALP	21.0 ± 0.8	-34.1 ± 1.3
AMLP	21.8 ± 0.9	-29.7 ± 2.4

[a] Mean ± SD (n=9)

Figure 1. Optical and physicochemical properties of fAuNPs. A) Absorbance spectra of 10 μM ALP and MLPs and their supernatants collected after reactions. B) Absorbance spectra of AuNPs (i), 10 μM AALPs (ii), 10 μM AMLPs (iii), 50 μM AALPs (iv), and 20 μM AMLPs (v). C) Hydrodynamic size and ζ–potential of AuNP and fAuNPs (AALPs and AMLPs).

HPLC, and their molecular weights were characterized by electrospray ionization (ESI; Supporting Information, Figure S1). To obtain optimal incorporation of LOAP incorporation, various concentrations of ALP or MLP were allowed to react with AuNPs. The LOAPs reacted rapidly with AuNPs through the C-terminal thiol group on the cysteine residue.[11,17] The number of LOAPs on each AuNP was calculated indirectly by measuring the absorbance of unbound LOAPs in solution. The optimal condition was determined to be 10 μM ALP or MLP reacting with AuNPs (7.0×10^{11} particles; Figure 1 and Supporting Information, Table S1). UV absorbance of the supernatants showed no detectable fluorescence intensity after centrifugation of the fAuNP solution (Figure 1A), indicating that all LOAPs bound to AuNPs. On average, approximately 8000 LOAPs were attached to each particle (**Table 1**).

Bare AuNPs (diameter of 20 nm) have a strong absorbance band at 520 nm. However, when concentrations of ALP or MLP were increased (>20 μM), the absorbance at near 630 nm also increased (Figure 1B). These red-shifted surface plasmon resonance (SPR) bands are commonly observed upon aggregation of AuNPs, which, in this study, was induced by excess amounts of LOAPs. A concomitant color change from red to dark blue with an extra broad band at 620–640 nm was observed in the presence of 20 μM MLP or 50 μM ALP.[12] This second band is characteristic of the interparticle coupling effect where AuNPs in close proximity possess a longitudinal SPR that absorbs light with longer wavelengths.[35,36]

Excess ALP or MLP induced immediate AuNPs aggregation because these peptides can bridge adjacent AuNPs as a common structural feature.[37] Aggregation occurs when the van der Waals attractive forces between AuNPs are greater than the electrostatic repulsive forces produced by the AuNP surface. The comparably long chain of the myristoyl acid in MLP induced more severe AuNP aggregation than the acetyl group in ALP. Recent studies have attempted to functionalize NPs with a stabilizing surface consisting of polyethylene glycol (PEG), protein, DNA, and others.[38,39] Although these stabilized NPs do not aggregate initially, several experiments have demonstrated delayed aggregation of NPs.[38,39]

The AuNPs functionalized with ALP or MLP were termed AALPs and AMLPs, respectively. Dynamic light scattering (DLS) measurements of the fAuNPs confirmed the above absorbance results. Single populations of AALPs (21.0 ± 0.8 nm) and AMLPs (21.8 ± 0.9 nm) were obtained with 10 μM ALP or MLP. The initial ζ–potential of bare AuNPs was –38.8 mV, but, the surface charges of AALPs and AMLPs changed to –34.1 mV and –29.7 mV, respectively, due to the positively charged oligoarginine residues. When the concentration of LOAPs increased, the DLS data revealed a broad size distribution with multiple size peaks (65–350 nm), indicating that the heterogeneous population was caused by different aggregations of fAuNPs (Supporting Information, Table S1). Consequently, fAuNPs conjugated with 10 μM ALP or MLP were used for the following cell studies.

Table 1. Fatty acids and peptide sequences of LOAPs used for surface modification of AuNPs.

Name	Sequence [a]	Mw ([M+H]+)	Mw (ESI)
ALP	Acetyl-βA(dR)$_{11}$K(FITC)C-SH	2468.33	2468.24
MLP	Myristoyl-βA(dR)$_{11}$K(FITC)C-SH	2636.52	2636.44

[a] βA for beta-alanine, dR for D-arginine.

2.2. Cellular Uptake of fAuNPs

Jurkat cells (3.5×10^4) were incubated with 3.5×10^8 AALPs or AMLPs for 4 h at 37 °C. Cells were then treated with trypsin to remove surface attached LOAPs that might interfere with intracellular fluorescein detection. As controls, cells were incubated with AuNPs (3.5×10^8 particles) or 5 nM LOAPs to determine non-specific background levels. The cellular uptake of fAuNPs was characterized by flow cytometry, and FITC fluorescence intensities were compared with those from unlabeled cells (UL; **Figure 2**). Compared to the fluorescence intensity of AALPs or AMLPs (solid line), the signal intensity of ALP or MLP (dashed line) showed right shifts, indicating that LOAPs could label Jurkat cells with high efficiency (Figure 2A). Much higher fluorescence intensity was obtained with MLP than ALP. It is well known that an improved cellular uptake can be achieved if appropriate hydrophobic lipid chains (C8 to C16) are anchored on peptides, suggesting the critical contribution of fatty acids in cellular trafficking activity.[28–32] Although the

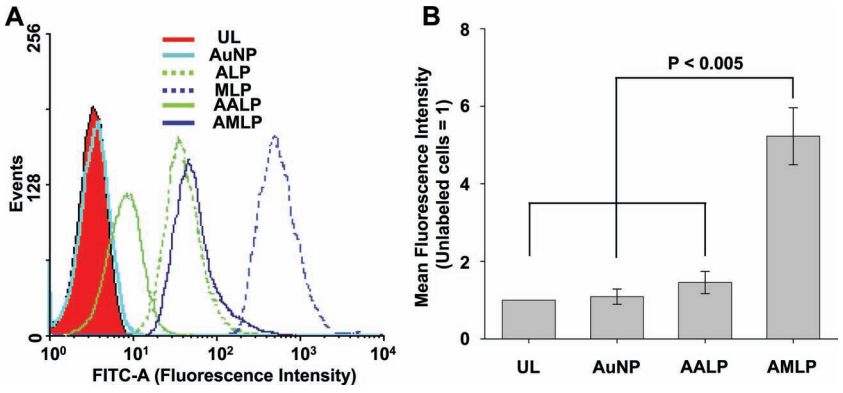

Figure 2. Cellular uptake of fAuNPs. Jurkat cells were incubated for 4 h at 37 °C with fAuNPs, washed, treated with trypsin, and analyzed by flow cytometry. A) Histogram profiles of cells treated with LOAPs and fAuNPs. Positively labeled cells are identified by FITC fluorescence signals, which originate from ALP (solid green), MLP (solid blue), AALPs (dotted green), or AMLPs (dotted blue). B) The mean fluorescence intensity of bare AuNPs and fAuNPs (AALPs and AMLPs). For comparison purposes, the fluorescence signal of unlabeled cells was set as the reference (UL = 1). Each experiment was performed at least three times in triplicate, and the results are expressed as the median change in fluorescence ± SD.

fluorescence intensity of fAuNPs was lower than it of free LOAPs, considerable cellular uptake of fAuNPs was achieved. Bare AuNPs did not exhibit any noticeable fluorescence signal due to the absence of FITC dyes. Mean fluorescence intensities of AALPs and AMLPs as well as bare AuNPs compared with UL are shown in Figure 2B. Cellular uptake of AALPs (1.46 ± 0.28 fold) was slightly greater than that of AuNPs (1.09 ± 0.2 fold) although the mean intensity did not reach statistical significance, whereas the cellular uptake of AMLPs was significantly increased (5.23 ± 0.73 fold; $P < 0.005$). Cellular uptake data indicate that fAuNPs conjugated with MLP enter Jurkat cells with a high efficiency, likely due to the myristoyl fatty acid group.

2.3. Cytotoxicity of fAuNPs

The potential cellular toxicity of fAuNPs was investigated after 4 h incubation in Jurkat cells using MTS assays.[40,41] Unlabeled cells served as a control, and their cell viabilities were set at 100% (**Figure 3**A). Cells treated with AALPs or AMLPs expressed similar viabilities as untreated or AuNP treated cells. A cell-permeant dye, calcein red-orange AM, was also used to assess cellular uptake and cell toxicity of fAuNPs in Jurkat cells. Cells were incubated for 4 h at 37 °C with AuNPs or fAuNPs to allow cellular uptake, treated with trypsin to remove surface bound LOAPs, and then incubated for 15 min at 37 °C with 1 μM calcein red-orange AM. The cells were washed with PBS and analyzed by flow cytometry. Band-pass emission filters, 530 ± 15 nm and 585 ± 21 nm, were

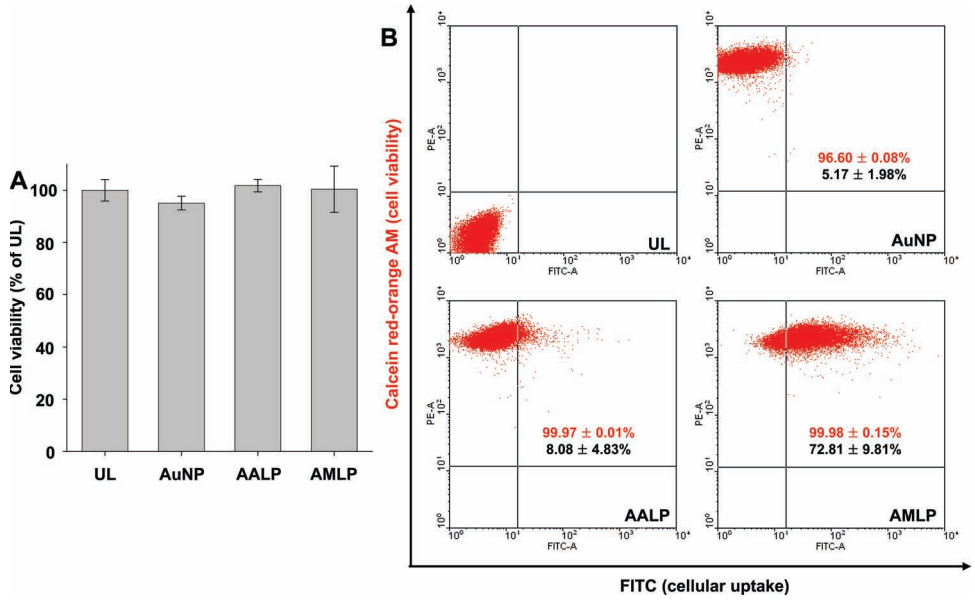

Figure 3. Cell viability and cellular uptake. A) Cell viability as assessed by MTS assay. Jurkat cells (3.5×10^4) were incubated for 4 h at 37 °C with AuNPs or fAuNPs (AALPs or AMLPs), washed with PBS, and treated with trypsin. Then 100 μL fresh culture media was added to each well. The plates were incubated for 4 h after the addition of 20 μL MTS/PMS solution to each well, and the absorbance was read at 490 nm. The background absorbance was determined in wells containing media (without cells) and was subtracted from the experimental values. The absorbance values were converted to percentage viability against control and reported as the mean and standard deviation. All experiments were repeated three times. B) Calcein red-orange AM-based cell viability and cellular uptake as measured by flow cytometry. Jurkat cells (3.5×10^4) were incubated for 4 h at 37 °C with AuNPs or fAuNPs (AALPs or AMLPs), washed with PBS, treated with trypsin, and resuspended in HBSS. Cells were then incubated for 10 min with 1 μM calcein red-orange AM. Cellular uptake and cell viability were analyzed by flow cytometry as described in the Experimental Section. Results are presented as representational dot plots of cell viability (SSC) versus cellular uptake (*FSC*).

used to detect FITC signal (cellular uptake; x-axis) and calcein red-orange signal (cell viability; y-axis), respectively. We found that more than 99% of cells incubated with AALPs and AMLPs were positive for calcein red-orange, indicating that they were viable (Figure 3B). These data suggest that neither the AuNPs nor fAuNPs used in the present study induce any measurable cell toxicity in Jurkat cells. Cells treated with AMLPs (72.81 ± 9.81%) had significantly improved cellular uptake ($P < 0.005$) compared with cells incubated with AALPs (8.08 ± 4.83%) or bare AuNPs (5.17 ± 1.98%).

We further investigated intracellular distribution and cellular toxicity of fAuNPs by observing FITC and calcein red-orange fluorescence in Jurkat cells via CLSM. Since the cell fixation process could cause artifacts in the intracellular distribution of cargo molecules, all microscopic observations were conducted in live cells.[31,42] Confocal microscopic images showed FITC and calcein red-orange were distributed inside the Jurkat cells (**Figure 4**). FITC fluorescence, which corresponded to FITC molecules conjugated to AALPs or AMLPs, was evenly distributed in the plasma membrane and cytoplasm (Figure 4B; intracellular distribution). Several small, punctuated spots were observed in the cytoplasmic membrane of cells treated with AMLPs, indicating that multiple pathways might be involved during cellular uptake and intracellular trafficking.[31,43] Calcein red-orange fluorescence images further demonstrated the lack of cellular toxicity of fAuNPs (Figure 4C; cell viability). There were no significant differences in calcein red-orange cellular fluorescence between AuNPs and fAuNPs. This indicates that AuNPs and fAuNPs did not compromise the Jurkat cells plasma membranes, because upon cleavage by intracellular esterases, calcein red-orange was retained in live cells that possess intact plasma membranes. Overlay images indicate that fAuNPs are localized in intracellular compartments and are non-toxic to cells (Figure 4D).

2.4. Dark-Field and Hyperspectral Microscopic Analysis of fAuNPs in Live Cells

The intracellular distribution of AuNPs and fAuNPs in MDA-MB-231 breast cancer cells was visualized using high contrast dark-field microscopy. This technique has been utilized to characterize the expression of scattered light from AuNPs because the plasmons enable imaging individual NP in cells, where only steady-state scattered light can be detected.[44,45] Cells (3.5×10^4) were seeded on 6-well chamber slides and incubated for 4 h at 37 °C with 3.5×10^8 AuNPs or fAuNPs. Cells were then treated with trypsin, washed with PBS,

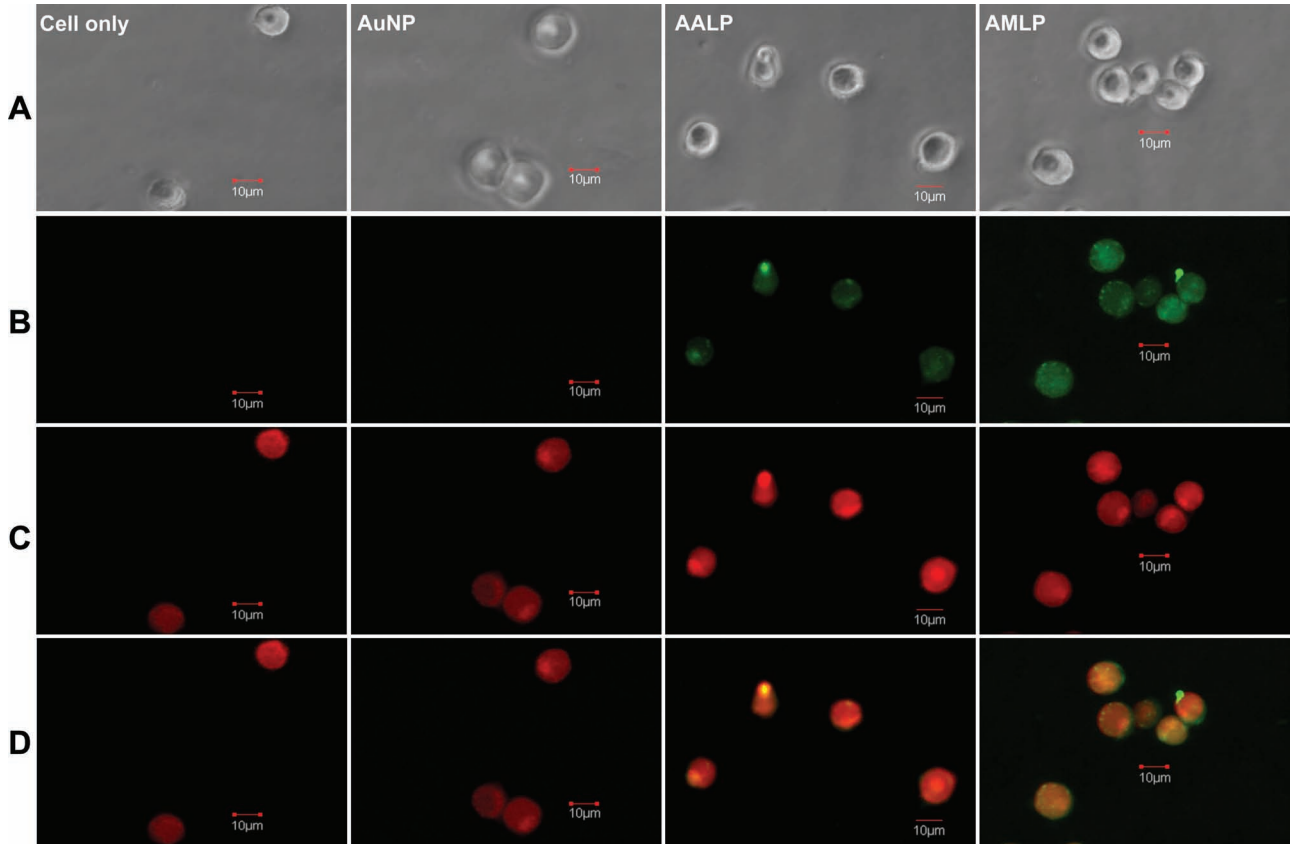

Figure 4. CLSM for cellular uptake of fAuNPs and subsequent cell viability. Cells were incubated with AuNPs or fAuNPs for 4 h,and then labelled with calcein red-orange AM dye. A) Bright field images. B) Images of intracellular delivered particles. C) Images of calcein red-orange AM to evaluate cell viability. D) Intracellular localization of particles (green) and calcein red-orange (red) colocalized (light orange) as shown in the merged overlay images. Fluorescence images were captured using an Olympus Fluo ViewTM 1000 CLSM using oil immersion 60× objective in culture slides with excitation by 488 nm (FITC) and 543 nm (calcein red-orange) laser lines, respectively.

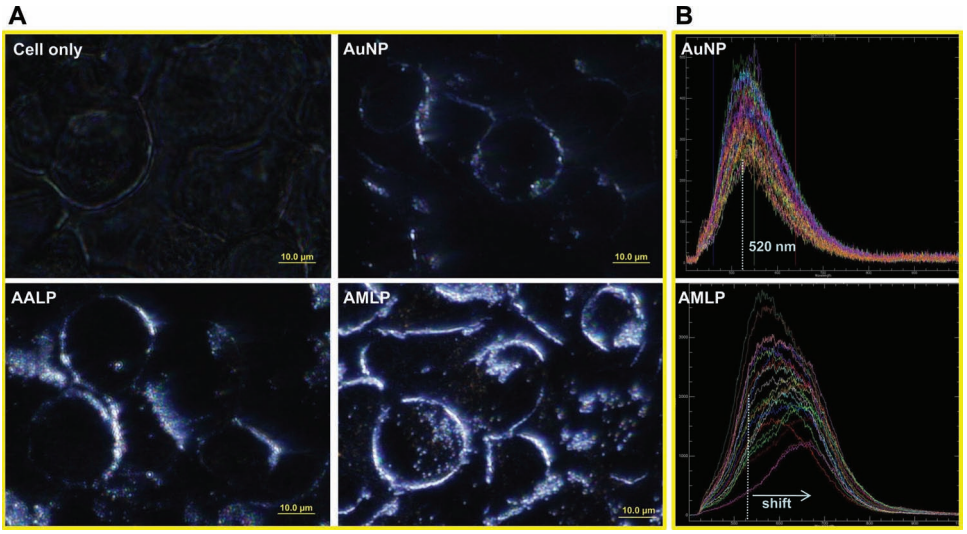

Figure 5. High contrast dark-field microscopic images and spectral profiles of MDA-MB-231 breast cancer cells. A) Cells (3.5×10^4) were incubated for 4 h at 37 °C with 3.5×10^8 AuNPs or fAuNPs. Untreated control cells are shown in upper left panel. Following treatment, cells in 6-well chamber slides were washed with PBS twice and imaged using dark-field microscopy. B) Spectral library of AuNPs (top) and AMLPs (bottom) were obtained from the CytoViva hyperspectral microscopy system.

resuspended in PBS, and observed via dark-field microscopy without cell fixation (**Figure 5**A). Most AuNPs and AALP failed to enter cells and were confined to cell plasma membrane. However, AMLPs were internalized and dispersed in both the plasma membrane and intracellular compartments. Spectral libraries of AuNPs and fAuNPs (AMLPs) were identified and mapped within a single-cell culture. To accomplish this, the AuNPs were first imaged independently and spectral profiles were created for each particle size (Figure 5B). The spectral profiles of AMLP showed far red shifts compared with those of AuNPs (≈520 nm), indicating multiple heterogeneous populations of intracellularly aggregated fAuNPs. This finding confirmed that, without physical rupture or fusion of the cell membrane, LOAPs are capable of delivering AuNPs directly into cells.

3. Conclusions

In conclusion, the MLP peptide, which consists of a myristoyl lipid moiety and an oligoarginine group, can facilitate intracellular delivery of AuNPs without detectable cellular toxicity. Although CPPs alone have been proven useful in transporting various NPs into cells,[6,7,11,17,25] ALP, which lacks a lipid domain, is much less effective than MLP in delivering AuNPs into cells. The cellular uptake of fAuNPs by live cells strongly depends on their surface functional groups. Presumably, the positive charges in the oligoarginine residues (R11) first interact with the negatively charged membrane. Then, the hydrophobic myristoyl chain enables fAuNPs to bind more tightly to the membrane and accelerates membrane translocation. Due to their relatively easy conjugation to drugs, low cell toxicity, and excellent optical and physical properties, MLP functionalized nanoparticles are expected to have great potentials in the areas of targeted drug delivery, cell imaging, cancer diagnostics, and hyperthermia cancer therapy.

4. Experimental Section

Surface Modification of AuNPs: AuNPs (20 nm, Ted Pella Inc., Redding, CA) were functionalized by conjugating acetylated oligoarginine (acetyl-dR11; ALP) or myristoylated oligoarginine (myristoyl-dR11; MLP), which were synthesized as reported previously.[30,31] Detailed information is available in the Methods Section of the Supporting Information. In brief, an acetyl (C2) or myristoyl (C14) group was conjugated to the N-terminal β-alanine residue of the oligo-d-arginine peptide (dR11). FITC was attached to the lysine side chain, and a C-terminal cysteine residue was introduced to provide a reactive thiol group for AuNP conjugation (Supporting Information, Scheme S1). ALP or MLP solutions (10–100 μM) were added to 1 mL AuNP solution (20 nm, 7×10^{11} particles.) and allowed to react for 10 min at room temperature with gentle shaking. The fAuNPs were then centrifuged at 12,000 g for 30 min, and the pellet was resuspended in PBS (1 mL). We acquired UV-visible absorption spectra of the fAuNPs and supernatants to screen whether aggregation occurred during modification and to determine the final concentration of fAuNPs by indirectly measuring the signal intensity of unbound ALP or MLP supernatants. From the standard volume, a known amount of solution was removed for absorbance measurements and the concentration of unbound LOAPs was calculated. The average number of LOAP molecules per particle after reacting with LOAP (10 μM) is approximately 8000.

fAuNPs Characterization: The physicochemical properties of the fAuNPs were evaluated by spectroscopy and ζ–potential measurements. UV-visible absorption and emission spectra were measured at room temperature using a Cary 50 Bio UV Spectrophotometer (Varian, Palo Alto, CA) at a 400–850 nm wavelength range with a slit width of 2 nm and 200 nm min^{-1} scan rates. Dynamic light scattering (DLS) and ζ–potential were measured using Malvern ZetaSizer Nano ZS (Worcestershire, UK) at a light source wavelength of 532 nm. DLS size distribution was analyzed by volume and ζ–potential distribution was analyzed by intensity.

Cell Cultures: Human Jurkat cells or MDA-MB-231 breast cancer cells were cultured in RPMI-1640 or DMEM supplemented with 10% FBS and 1% penicillin/streptomycin. Cells were grown in 75 cm^2 culture flasks at 37 °C in a 5% CO_2 incubator. The culture media was changed every 3 days until cells were nearly confluent. The cells were then further incubated in various culture conditions depending on the experiment (cellular uptake characterization, intracellular fate evaluation, or cell toxicity).

Flow Cytometric Analyses: To evaluate cellular uptake of LOAPs or fAuNPs, Jurkat cells (3.5×10^4) were incubated for 4 h at 37 °C with fAuNPs (3.5×10^8) or LOAPs (5 μM). Cells were thoroughly washed with PBS and then incubated for 5 min at 37 °C with trypsin-EDTA (200 μL) to remove LOAPs or fAuNPs bound to the cell surface. At the end of trypsin treatment, 200 μL culture media was added to neutralize the protease. A total of 2×10^4 events were recorded using FACS LSR II (BD Biosciences, Franklin Lakes, NJ) and analyzed by WinMDI software (The Scripps Institute, La Jolla, CA).

MTS Cell Viability Assay: The CellTiter 96 aqueous non-radioactive cell proliferation assay (Promega, Madison, WI) was used following the manufacturer's instructions. Jurkat cells (3.5×10^4) were suspended in phenol free RPMI 1640 (200 μL) with FBS (10%) and incubated overnight at 37 °C and 5% CO_2 in 96-well plates. The cells were treated for 4 h with 3.5×10^8 bare AuNPs or fAuNPs. The negative control was cell only (in the absence of NPs). After washing the cells twice with PBS, 100 μL fresh culture media was added to each well. The plates were incubated for 4 h after 20 μL of the combined MTS/PMS solution was added to each well and the absorbance was read at 490 nm using a SpectraMax M2 Microplate reader (Molecular Devices Inc., Sunnyvale, CA). All experiments were repeated three times.

Cell Viability and Cellular Uptake Using Calcein Orange-Red AM Dye: Jurkat cells (3.5×10^4) were treated for 4 h with 3.5×10^8 bare AuNPs or fAuNPs. After washing the cells twice with Hank's buffered salt solution (HBSS; Gibco, Grand Island, NY), 500 μL culture media was added to each well. Cells were then labeled for 30 min at 37 °C with CellTrace calcein red-orange AM (1.0 mM, Molecular Probes, Eugene, OR), washed thoroughly with HBSS to minimize background, and then incubated for 5 min at 37 °C with trypsin-EDTA (200 μL). Culture media (200 μL) was added to neutralize the trypsin. The cells were resuspended in HBSS (400 μL) and sorted using a FACS LSR II (BD Biosciences) equipped with a 488 nm argon-ion laser (2×10^4 events). A 530 ± 15 nm band pass filter was used to detect the FITC green stain signal, and a 585 ± 21 nm band pass filter was used to detect the calcein red-orange AM signal. To observe fAuNPs cellular uptake, cells suspended in HBSS were transferred to culture slides. Images were obtained using a Olympus Fluo View 1000 CLSM (Center Valley, PA) with an oil immersion 60× objective and 488 nm (FITC) and 577 nm (calcein red-orange) excitation with an argon laser line. FV 1000 Viewer was used for image analysis.

Images and Spectral Library of AuNPs: MDA-MB-231 breast cancer cells (3.5×10^4) were cultured overnight at 37 °C and 5% CO_2 in 6-well chamber slides with DMEM and 10% FBS. Cells were treated for 4 h at 37 °C with 100 nM AuNPs or fAuNPs, and then washed with PBS. Images of AuNPs and fAuNPs in cells were directly observed by high contrast BX 50 dark-field microscopy (Olympus) using a 60× oil immersion objective. The spectral library of AuNPs and fAuNPs was obtained from CytoViva Hyperspectral Microscope system (Auburn, AL).

Statistical Analyses: Statistical comparisons of particle size, ζ–potential, cellular uptake, and cell viability were evaluated by paired-sample Student t-tests. Differences were considered statistically significant at $P < 0.05$, and each experiment was performed at least three times. The results are expressed as the mean ± SD.

Supporting Information

Supporting Information is available from the Wiley Online Library or from the author.

Acknowledgements

This research was supported in part by NIH CA135312. The authors would like to thank CytoViva for supporting the hyperspectral library of AuNPs (www.cytoviva.com).

Received: May 17, 2012
Published online: July 27, 2012

[1] I. H. El-Sayed, X. Huang, M. A. El-Sayed, *Nano Lett.* **2005**, *5*, 829.
[2] W. Jiang, B. Y. Kim, J. T. Rutka, W. C. Chan, *Nat. Nanotechnol.* **2008**, *3*, 145.
[3] A. Asati, S. Santra, C. Kaittanis, J. M. Perez, *ACS Nano* **2010**, *4*, 5321.
[4] T. Kanazawa, Y. Takashima, M. Murakoshi, Y. Nakai, H. Okada, *Int. J. Pharm.* **2009**, *379*, 187.
[5] J. K. Jaiswal, H. Mattoussi, J. M. Mauro, S. M. Simon, *Nat. Biotechnol.* **2003**, *21*, 47.
[6] M. Lewin, N. Carlesso, C. H. Tung, X. W. Tang, D. Cory, D. T. Scadden, R. Weissleder, *Nat. Biotechnol.* **2000**, *18*, 410.
[7] L. Josephson, C. H. Tung, A. Moore, R. Weissleder, *Bioconjugate Chem.* **1999**, *10*, 186.
[8] I. H. El-Sayed, X. Huang, M. A. El-Sayed, *Cancer Lett.* **2006**, *239*, 129.
[9] L. R. Hirsch, R. J. Stafford, J. A. Bankson, S. R. Sershen, B. Rivera, R. E. Price, J. D. Hazle, N. J. Halas, J. L. West, *Proc. Natl. Acad. Sci. USA* **2003**, *100*, 13549.
[10] B. D. Chithrani, W. C. Chan, *Nano Lett.* **2007**, *7*, 1542.
[11] R. Levy, N. T. Thanh, R. C. Doty, I. Hussain, R. J. Nichols, D. J. Schiffrin, M. Brust, D. G. Fernig, *J. Am. Chem. Soc.* **2004**, *126*, 10076.
[12] P. Nativo, I. A. Prior, M. Brust, *ACS Nano* **2008**, *2*, 1639.
[13] S. K. Lee, M. S. Han, S. Asokan, C. H. Tung, *Small* **2011**, *7*, 364.
[14] S. H. Wang, C. W. Lee, A. Chiou, P. K. Wei, *J. Nanobiotechnol.* **2010**, *8*, 33.
[15] M. Liang, I. C. Lin, M. R. Whittaker, R. F. Minchin, M. J. Monteiro, I. Toth, *ACS Nano* **2010**, *4*, 403.
[16] E. C. Cho, J. Xie, P. A. Wurm, Y. Xia, *Nano Lett.* **2009**, *9*, 1080.
[17] S. Pujals, N. G. Bastus, E. Pereiro, C. Lopez-Iglesias, V. F. Puntes, M. J. Kogan, E. Giralt, *ChemBioChem* **2009**, *10*, 1025.
[18] A. G. Tkachenko, H. Xie, Y. Liu, D. Coleman, J. Ryan, W. R. Glomm, M. K. Shipton, S. Franzen, D. L. Feldheim, *Bioconjugate Chem.* **2004**, *15*, 482.
[19] A. G. Tkachenko, H. Xie, D. Coleman, W. Glomm, J. Ryan, M. F. Anderson, S. Franzen, D. L. Feldheim, *J. Am. Chem. Soc.* **2003**, *125*, 4700.
[20] A. D. Petrescu, A. Vespa, H. Huang, A. L. McIntosh, F. Schroeder, A. B. Kier, *Biochim. Biophys. Acta* **2009**, *1788*, 425.
[21] E. M. Barnett, X. Zhang, D. Maxwell, Q. Chang, D. Piwnica-Worms, *Proc. Natl. Acad. Sci. USA* **2009**, *106*, 9391.
[22] D. Maxwell, Q. Chang, X. Zhang, E. M. Barnett, D. Piwnica-Worms, *Bioconjugate Chem.* **2009**, *20*, 702.
[23] C. H. Tung, R. Weissleder, *Adv. Drug Delivery Rev.* **2003**, *55*, 281.
[24] V. P. Torchilin, R. Rammohan, V. Weissig, T. S. Levchenko, *Proc. Natl. Acad. Sci. USA* **2001**, *98*, 8786.
[25] J. M. de la Fuente, C. C. Berry, *Bioconjugate Chem.* **2005**, *16*, 1176.
[26] S. Futaki, T. Suzuki, W. Ohashi, T. Yagami, S. Tanaka, K. Ueda, Y. Sugiura, *J. Biol. Chem.* **2001**, *276*, 5836.
[27] D. J. Mitchell, D. T. Kim, L. Steinman, C. G. Fathman, J. B. Rothbard, *J. Pept. Res.* **2000**, *56*, 318.
[28] S. Futaki, W. Ohashi, T. Suzuki, M. Niwa, S. Tanaka, K. Ueda, H. Harashima, Y. Sugiura, *Bioconjugate Chem.* **2001**, *12*, 1005.
[29] J. Fernandez-Carneado, M. J. Kogan, N. Van Mau, S. Pujals, C. Lopez-Iglesias, F. Heitz, E. Giralt, *J. Pept. Res.* **2005**, *65*, 580.
[30] W. Pham, M. F. Kircher, R. Weissleder, C. H. Tung, *ChemBioChem* **2004**, *5*, 1148.
[31] J. S. Lee, C. H. Tung, *Mol. Biosyst.* **2010**, *6*, 2049.
[32] J. S. Lee, C. H. Tung, *Biopolymers* **2011**, *96*, 772.
[33] S. Keller, I. Sauer, H. Strauss, K. Gast, M. Dathe, M. Bienert, *Angew. Chem. Int. Ed.* **2005**, *44*, 5252.
[34] A. Harishchandran, R. Nagaraj, *Biochim. Biophys. Acta* **2005**, *1713*, 73.
[35] S. K. Ghosh, T. Pal, *Chem. Rev.* **2007**, *107*, 4797.

[36] S. Basu, S. K. Ghosh, S. Kundu, S. Panigrahi, S. Praharaj, S. Pande, S. Jana, T. Pal, *J. Colloid Interface Sci.* **2007**, *313*, 724.
[37] A. Albanese, W. C. Chan, *ACS Nano* **2011**, *5*, 5478.
[38] F. K. van Landeghem, K. Maier-Hauff, A. Jordan, K. T. Hoffmann, U. Gneveckow, R. Scholz, B. Thiesen, W. Bruck, A. von Deimling, *Biomaterials* **2009**, *30*, 52.
[39] K. Rausch, A. Reuter, K. Fischer, M. Schmidt, *Biomacromolecules* **2010**, *11*, 2836.
[40] E. E. Connor, J. Mwamuka, A. Gole, C. J. Murphy, M. D. Wyatt, *Small* **2005**, *1*, 325.
[41] J. M. de la Fuente, C. C. Berry, M. O. Riehle, A. S. Curtis, *Langmuir* **2006**, *22*, 3286.
[42] J. P. Richard, K. Melikov, E. Vives, C. Ramos, B. Verbeure, M. J. Gait, L. V. Chernomordik, B. Lebleu, *J. Biol. Chem.* **2003**, *278*, 585.
[43] S. El-Andaloussi, H. J. Johansson, T. Holm, U. Langel, *Mol. Ther.* **2007**, *15*, 1820.
[44] A. Curry, W. L. Hwang, A. Wax, *Opt. Express* **2006**, *14*, 6535.
[45] C. Yu, H. Nakshatri, J. Irudayaraj, *Nano Lett.* **2007**, *7*, 2300.